Article published online: 2022-03-31

Design, Synthesis, and Evaluation of Benzoheterocyclic-Containing Derivatives as Novel HDAC1 Inhibitors

Min-Ru Jiao[1] Bo Han[1] Xiu Gu[1,2] Hao Zhang[1] Ai-Ping Wang[3] Qing-Wei Zhang[1*]

[1] Novel Technology Center of Pharmaceutical Chemistry, Shanghai Institute of Pharmaceutical Industry Co., Ltd., China State Institute of Pharmaceutical Industry, Shanghai, People's Republic of China
[2] School of Chemistry and Chemical Engineering, Shanghai University of Engineering Science, Shanghai, People's Republic of China
[3] Qingdao Yingli Medical Equipment Co., Ltd., Qingdao, People's Republic of China

Address for correspondence Qing-Wei Zhang, PhD, Novel Technology Center of Pharmaceutical Chemistry, Shanghai Institute of Pharmaceutical Industry Co., Ltd., 285 Gebaini Road, Shanghai 201203, People's Republic of China (e-mail: sipiqingwei@163.com).

Pharmaceut Fronts 2022;4:e22–e29.

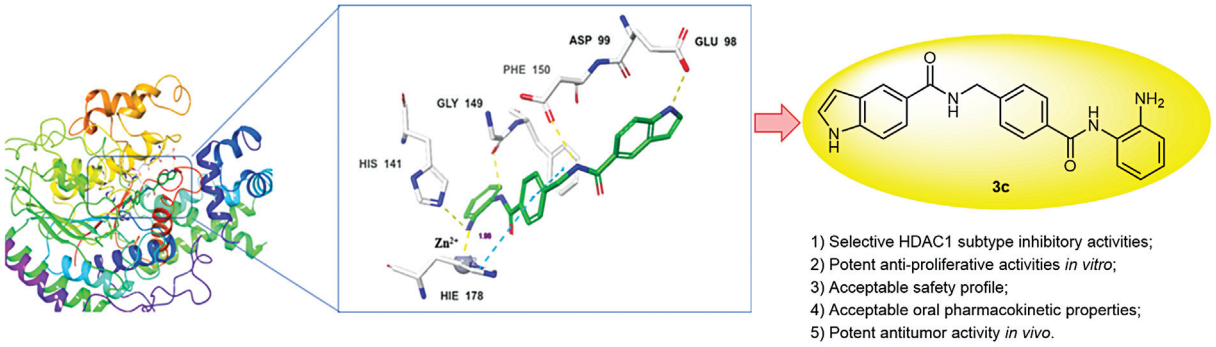

Abstract

In this study, the synthesis and biological evaluation of a variety of benzoheterocyclic-containing benzamide derivatives were described. Some of these compounds were proved to inhibiting the activity of histone deacetylase 1 (HDAC1) with IC_{50} values below the micromolar range, retarding proliferation of several human cancer cells, and surprisingly, not possessing toxicity to human normal cells and hERG K^+ ion channels. Among those compounds, **3c** was the most potent and efficacious derivative. Compound **3c** was orally active and displayed excellent *in vivo* antitumor activity in a HCT-116 xenograft mice model.

Keywords
- benzamide derivatives
- HDAC1 inhibitors
- orally active
- antitumor activity

Introduction

Histone deacetylases (HDACs) and histone acetyltransferases jointly regulate the acetylation levels of cellular histone proteins, thereby regulating the expression of genes. At present, 18 human HDACs have been identified and divided into four classes: Class I (HDAC1, HDAC2, HDAC3, and HDAC8), Class II (HDAC4, HDAC5, HDAC6, HDAC7, HDAC9, and HDAC10), Class III (SIRT1–7), and Class IV (HDAC11).[1,2] The overexpression of HDACs is closely associated with cancers, neurological diseases, inflammatory diseases, metabolic disorders, etc.[3,4] The development of HDAC inhibitors (HDACIs) has become a promising therapeutic strategy targeting these diseases, especially for cancers. Up to date, four HDACIs, namely vorinostat

received
November 15, 2021
accepted
January 29, 2022

DOI https://doi.org/10.1055/s-0042-1743487.
ISSN 2628-5088.

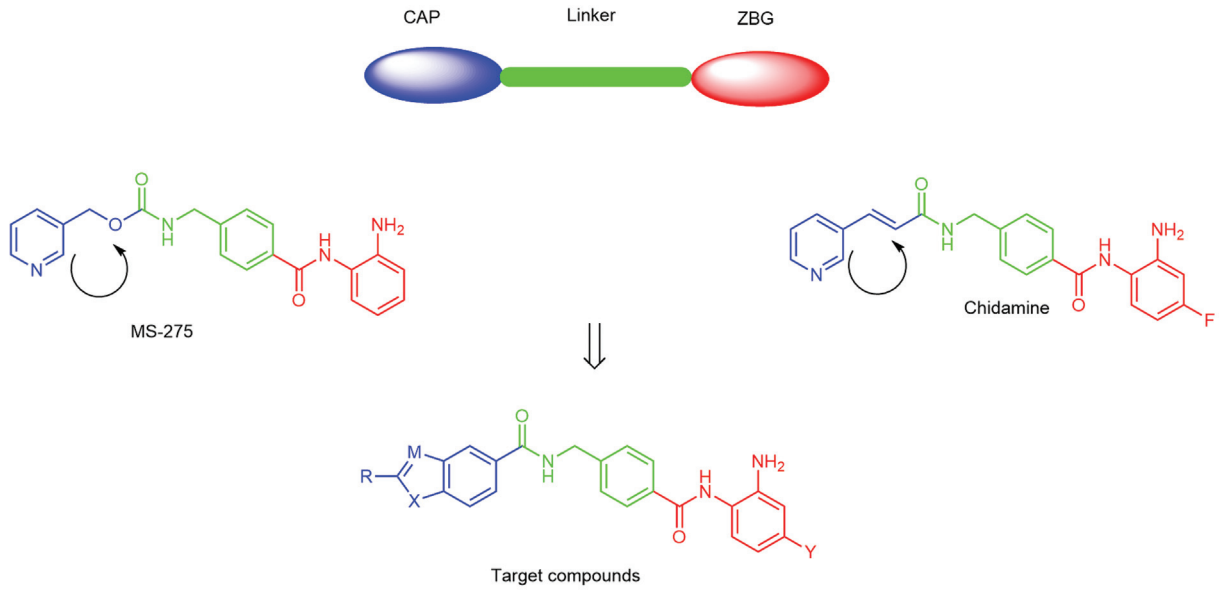

Fig. 1 Functional domains of benzamide HDACIs. HDACIs, histones deacetylase inhibitors.

(Zolinza; 2006), romidepsin (Istodax; 2009), belinostat (Beleodaq; 2014), and panobinostat (Farydak; 2015), have been approved by the U.S. Food and Drug Administration for cancer treatment.[5] However, most of the used HDACIs are of low selectivity, and may inhibit all or at least a few members of the HDAC family, leading to many side effects, low potency, or low stability during therapy.[6,7] Nowadays, a lot of benzamide-based HDACIs have entered clinical evaluation for the treatment of solid tumors and hematological malignancies, such as entinostat (MS-275), chidamide (CS055), and mocetinostat (MGCD0103).[8,9] They can selectively and significantly inhibit HDACs 1–3. Chidamide was the first orally available benzamide class of HDACIs approved by the China Food and Drug Administration for the treatment of advanced peripheral T cell lymphoma. MS-275 is another benzamide-based HDACI that preferentially inhibits HDAC1 ($IC_{50} = 510$ nmol/L) over HDAC3 ($IC_{50} = 1.7$ μmol/L). It showed good anticancer efficacy in experiments.[10] Above all, benzamide derivatives are research hotspots for exploring HDACIs.

Although there are various structural features for HDACIs, most HDACIs can be widely described with a zinc-binding group (ZBG), a linker, and a cap group (CAP) as shown in ►**Fig. 1**.[11] The structural similarity of the existing benzamide HDACIs suggested that rational isosteric modification of the surface-recognition domain or ZBG is feasible. By analyzing the structure–activity relationship of HDACIs (MS-275 and chidamide), herein we reported the design, synthesis, and preliminary bioactivity evaluation of benzoheterocyclic-containing benzamide derivatives as HDACIs (►**Fig. 1**).

Results and Discussion

The preparation of target compounds **3a–3n** is shown in **Scheme 1**. The intermediates **2a–2g** could be obtained by condensation of **1a–1g** and 4-aminomethyl-benzoic acid under the conditions of *O*-benzotriazol-1-yl-tetramethyluronium hexafluorophosphate (HBTU). Then intermediates **2a–2g** coupled with HBTU and further reacted with phenylenediamine or 4-fluorophenylenediamine to obtain the target compounds **3a–3n**. All synthetic compounds **3a–3n** are confirmed by ^{1}H NMR (nuclear magnetic resonance) and ESI-MS (electrospray ionization mass spectrometry).

The inhibitory effects of compounds **3a–3n** against HDAC1 enzyme subtype were determined by using a fluorescence-based assay as described before.[12] Data are presented as IC_{50} values in ►**Table 1**. The results showed that all the compounds showed potent HDAC1 inhibitory activity, but not significantly superior to chidamide except for compound **3c**. Compound **3c** exhibited a much smaller IC_{50} value (0.64 μmol/L) than that of chidamide ($IC_{50} = 1.28$ μmol/L)

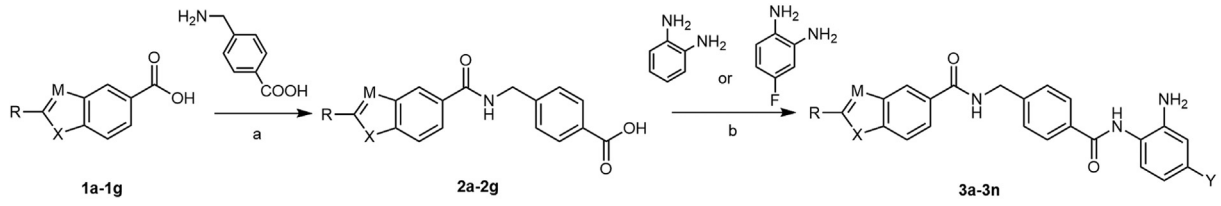

Scheme 1 Synthesis of compounds **3a–3n**. Reagent and conditions: (a) HBTU, TEA, r.t., NaOH (aq), 4 hours, CH_3CN; HCl (aq), pH = 5–6; (b) HBTU, TEA, DMF, r.t., 6 hours.

Table 1 The chemical structures and HDAC1 inhibitory activities of target compounds 3a–3n

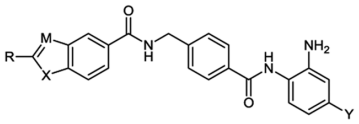

Compound	R	M	X	Y	HDAC1 IC_{50} (μmol/L)[a]
3a	H	N	NH	H	8.89
3b	H	N	NH	F	19.7
3c	H	CH	NH	H	0.640
3d	H	CH	NH	F	3.28
3e	CH_3	N	NH	H	17.5
3f	CH_3	N	NH	F	65.0
3g		N	NH	H	6.05
3h		N	NH	F	41.2
3i		N	NH	H	4.05
3j		N	NH	F	10.5
3k	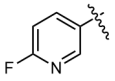	N	NH	F	9.02
3l	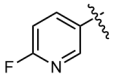	N	NH	H	3.23
3m	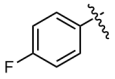	N	NH	F	20.8
3n	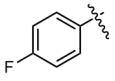	N	NH	H	7.63
Chidamide	–				1.28

[a]IC_{50} values are reported as the average of at least two separate determinations.

(►**Table 1**). As such, compound **3c** was used for the following study. As presented in ►**Table 1**, analogs containing the 2-amino-4-fluorophenyl group in the ZBG positions, such as **3b**, **3d**, **3f**, **3h**, **3j**, **3k**, and **3m**, were typically less potent than the derivatives with 2-aminophenyl substitution at the same position (**3a**, **3c**, **3e**, **3 g**, **3i**, **3l**, and **3n**). The introduction of more N atoms in the CAP region was not conducive to HDAC1 inhibitory activity of the compound (such as **3a** versus **3c**), suggesting that the electrostatic properties of the substitutions on the "CAP" group may play a critical role to contribute HDAC1 inhibitory activities.

To further understand the interaction between **3c** and HDAC1, molecular docking studies were performed to evaluate the possible binding modes of **3c** with the active site of HDAC1 (PDB entry: 4BKX) using Syble/FlexX module.[13] The docking results showed that compound **3c** could well insert into HDAC1 active sites (►**Fig. 2**). The benzamide group of compound **3c** could chelate the Zn^{2+} very well (1.96 Å to the nitrogen atom in aniline) in a bidentate fashion. Besides, four amino groups formed four hydrogen-bonding interactions with ASP-99 and GLY-149, respectively. In general, the result of molecular docking supported a tight interaction between compound **3c** and HDAC1.

MTT assay was further performed to assess the antiproliferative activity of **3c** in human cancer cell lines (PC-3, HT-29, HCT-116, SK-BR-3, Jurkat E6–1, A549, Colo205, and MCF-7) and human fetal lung fibroblast normal cell line (MRC-5).[14] ►**Table 2** demonstrates that compound **3c** presented better antiproliferative activity in most tested cancer cell lines with IC_{50} values obviously superior to chidamide, yet, a weak inhibitory activity against human normal cell MRC-5 cell lines ($IC_{50} > 10$ μmol/L), suggesting that compound **3c** inhibits

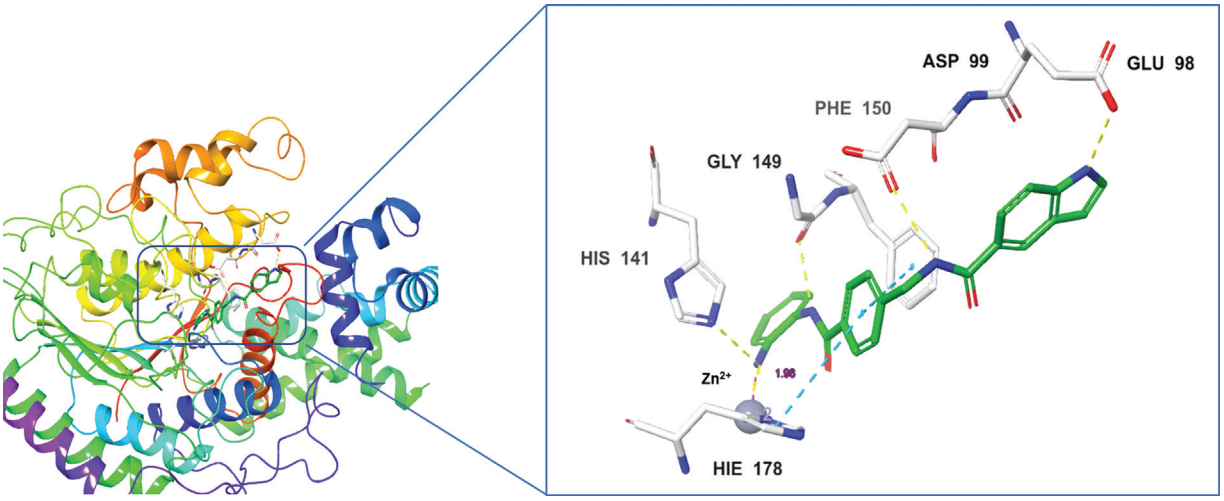

Fig. 2 Predicted binding modes of compound **3c** (carbon in *green*) with HDAC1 (PDB entry: 4BKX). *Yellow lines* stands for hydrogen bonds; *cyan lines* stands for π–π stacking.

Table 2 Antiproliferative activity of compound 3c

Compound	IC_{50} (μmol/L)[a]								
	PC-3	HT-29	HCT-116	SK-BR-3	Jurkat E6–1	A549	Colo205	MCF-7	MRC-5
3c	0.0549	0.148	0.0126	0.0337	0.0214	2.10	0.651	1.023	>10
Chidamide	1.07	0.168	0.381	0.139	0.0725	0.807	1.92	1.749	NT

[a]IC_{50} values are reported as the average of at least two separate determinations.

proliferation of cancer cells with desirable selectivity over human normal MRC-5 cell lines.

The selective inhibitory effect of compound **3c** for HDAC isoforms, including HDAC1 (Class I), HDAC8 (Class I), and HDAC6 (Class IIb), was also assessed (►**Table 3**). We found that **3c** showed potent inhibitory activity toward HDAC1 and HDAC2 ($IC_{50} = 2.1$ μmol/L) while weak activity against HDAC6 ($IC_{50} > 10$ μmol/L) and HDAC8 ($IC_{50} > 10$ μmol/L). Further, we investigated the cardiac safety of compound **3c** through a patch-clamp hERG K^+ channel screening. The results showed that **3c** was inactive in our hERG binding assay ($IC_{50} > 30$ μmol/L), demonstrating that the potential risk cardiotoxicity of **3c** was relatively low. The acute toxicity of compound **3c** was tested in ICR mice by oral administration. The result suggested that administration of **3c** at or below 1,500 mg/kg (po [oral]) may be safe for mice.

The pharmacokinetic study of **3c** was evaluated using Sprague-Dawley (SD) rats after single ig (intragastric) at 10 mg/kg and iv (intravenous) at 2 mg/kg. The C_{max} of **3c** was 5,260 μg/L after iv dosing for 0.05 hours. After ig dosing of **3c**, it was well cleared (CL = 6.26 L/h/kg) in rats and the terminal phase half-life of **3c** was 3.23 hours. Meanwhile, **3c** was well distributed ($V_z = 29.10$ L/kg) and the oral bioavailability was moderate (F = 10.35%) in rats (►**Table 4**). Therefore, research focus on enhancing the oral bioavailability of **3c** through exploring the novel formulation was further studied in our laboratory. Unfortunately, data are unavailable at present.

The antitumor activity of compound **3c** was further tested in a HCT-116 mouse xenograft model at daily intragastric doses of 45, 80, and 150 mg/kg for 28 days (►**Fig. 3**). It is apparent that **3c** inhibited tumor growth *in vivo*. Under the dose of 45, 80, and 150 mg/kg, the ratio of tumor volume in treated versus control mice (T/C) was 73.22, 71.01, and 43.43%, respectively, suggesting the obvious antitumor activity of compound **3c** *in vivo*.

Table 3 Roles of compound 3c in HDAC isoform activities and hERG binding, and its MTD value in ICR mice

Compound	IC_{50} (μmol/L)[a]				hERG IC_{50} (μmol/L)[b]	MTD (mg/kg)
	HDAC1	HDAC2	HDAC6	HDAC8		
3c	0.64	2.1	>10	>10	>30	>1,500

Abbreviation: MTD, maximum tolerance dose.
[a]IC_{50} values are reported as the average of at least two separate determinations.
[b]hERG patch clamp screen as described in a reported study.[12]

Table 4 Pharmacokinetic parameters of compound 3c[a]

Parameter	10 mg/kg (ig)	2 mg/kg (iv)
$AUC_{(0\text{-}t)}$ (μg/L × h)	1,686.6	3,260.1
$AUC_{(0\text{-}\infty)}$ (μg/L × h)	1,719.1	3,262.6
$MRT_{(0\text{-}\infty)}$ (h)	5.19	0.87
$t_{1/2}$ (h)	3.23	1.49
T_{max} (h)	1.5	0.05
CL (L/h/kg)	6.26	0.61
V_z (L/kg)	29.10	1.32
C_{max} (μg/L)	309.5	5,260
F (%)	10.35	

Abbreviations: AUC, area under the curve; CL, clearance; C_{max}, maximum concentration; F, bioavailability; MRT, mean residence time; $t_{1/2}$, elimination half-life; T_{max}, time to reach maximum concentration; V_z, distribution volume.

[a]For pharmacokinetic study, blood was collected from rats at various time points up to 24 hours, and plasma samples were analyzed using an Agilent 1200 HPLC system coupled with an Agilent 6410B triple–quadruple mass spectrometer. A solution of 0.05 N HCl in saline was used as the vehicle for both intravenous and intragastric dosing.

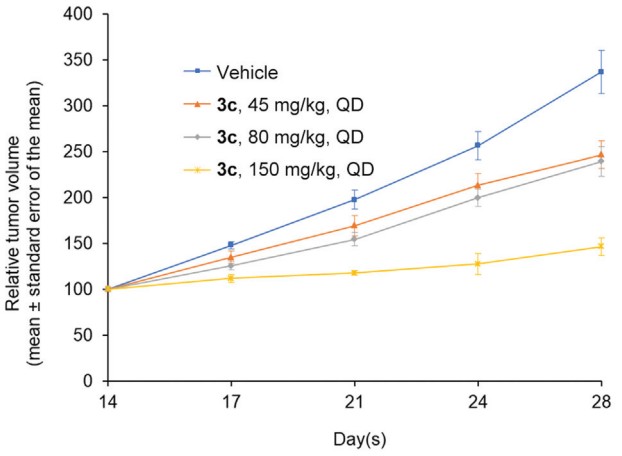

Fig. 3 Antitumor activity of **3c** in a mouse xenograft model.

Conclusion

We designed and synthesized 14 novel benzamide HDAC1 inhibitors. By screening inhibitory activity of HDAC1 and cellular antiproliferative activity, we found that compound **3c** possessed better inhibitory activities of HDAC1 and cellular antiproliferative activity superior to chidamide. Moreover, our data suggested that **3c** did not possess significant toxicity to primary human cells and the patch clamp hERG K^+ ion channel. Compound **3c** had good selectivity for HDAC1 over HDAC6 and HDAC8. The oral pharmacokinetic parameters of **3c** were acceptable. Results from *in vivo* antitumor activity study showed that **3c** exhibited potent oral antitumor activity in an HCT116 human colon carcinoma mouse xenograft model. Further assessment of compound **3c** is in progress and we will report in the future.

Experimental Section

Chemicals and Instruments

Unless otherwise noted, all solvents and reagents were commercially available (Bidepharm, Shanghai, People's Republic of China) and used without further purification. All reactions were monitored by thin-layer chromatography (TLC) on 0.25 mm silica gel plates (60 GF-254) and visualized with ultraviolet light (Shanghai Heqi Glassware Co., Ltd., People's Republic of China) or iodine vapor (Sinopharm Chemical Reagent Co., Ltd., People's Republic of China). ^{1}H NMR spectra were obtained using a Bruker DRX spectrometer (Bruker Co., Ettlingen, Germany) at 400 MHz. Chemical shifts were reported in parts per million (ppm). Multiplicity of ^{1}H NMR signals was reported as single (s), double (d), triplet (t), quarter (q), and multiplet (m). ESI-MS was determined on an API 4000 spectrometer (Applied Biosystems, Foster City, California, United States) with a turbo ion spray interface. Melting points were determined on an Electrothermal IA9200 melting point apparatus (Bibby-Electrotherma, United Kingdom) and were uncorrected. HPLC (high-performance liquid chromatography) analysis was performed on Agilent 1200 (Agilent Technologies, California, United States) with an extended C18 column (4.6 mm × 250 mm, 5 μm). The flow rate is 1 mL/min. All final compounds achieved a minimum of 95% purity.

General Synthetic Procedure of 3a–3n

To a suspension of HBTU (3.03 g, 8 mmol) in CH_3CN (5 mL) was added the corresponding **1a–1 g** (8.0 mmol) in CH_3CN (5 mL), and the mixture was stirred for 1.5 hours at room temperature (r.t.). The resulting solution was added to a solution of NaOH (0.32 g, 8 mmol) and 4-(aminomethyl)-benzoic acid (1.21 g, 8 mmol) in water (100 mL). After stirring for 4 hours at r.t., the solution was acidized with HCl (pH 5) to precipitate a white solid which was collected by filtration, washed with water (100 mL) and methanol (50 mL), respectively, and dried to give the benzoic acid derivatives **2a–2 g** without further purification. To a solution of the corresponding benzoic acid derivatives **2a–2 g** (1 equiv.) in DMF was added 1,2-phenylenediamine or 4-fluorophenylenediamine (1 equiv.), HBTU (1.2 equiv.), and TEA (4 equiv.) dropwise. The reaction mixture was stirred at r.t. for 6 hours, after which TLC analysis indicated the reaction was completed. The solution was added with water (20 equiv.) to precipitate a white solid. The mixture was poured into water and stirred for 30 minutes. Insoluble material was filtered. The solid was collected and dried to be recrystallized in aqueous ethanol to give target compounds **3a–3n**.

N-(4-((2-aminophenyl)carbamoyl)benzyl)-1*H*-benzo[*d*]imidazole-5-carboxamide (**3a**): Mp 165.3–167.9°C; ESI-MS (*m/z*): calcd. for $C_{22}H_{19}N_5O_2$ $[M+H]^+$ 386.1539; found 386.1643. ^{1}H NMR (400 MHz, DMSO-d_6) δ 11.24 (s, 1H), 9.64 (s, 1H), 8.34 (t, J = 16.0 Hz, 1H), 8.12 (s, 1H), 7.95 (d, J = 8.0 Hz, 2H), 7.78 (m, 1H), 7.72 (d, J = 8.0 Hz, 1H), 7.6 (d, J = 8.0 Hz, 1H), 7.47 (d, J = 8.0 Hz, 2H), 7.17 (d, J = 8.0 Hz, 1H), 6.97 (dt, J = 4.0, 8.0 Hz, 1H), 6.78 (d, J = 8.0 Hz, 1H), 6.60 (t, J = 8.0 Hz, 1H), 4.90 (s, 2H), 4.58 (d, J = 8.0 Hz, 2H).

N-(4-((2-amino-4-fluorophenyl)carbamoyl)benzyl)-1*H*-benzo[*d*]imidazole-5-carboxamide (**3b**): Mp 184.7–185.9°C. ESI-MS (*m*/*z*): calcd. for $C_{22}H_{18}FN_5O_2$ $[M+H]^+$ 404.1445; found 404.1497. ^{1}H NMR (400 MHz, DMSO-d_6) δ 9.57 (s, 1H), 9.12 (t, $J=8.0$ Hz, 1H), 8.34 (m, 1H), 8.12 (s, 1H), 7.95 (d, $J=8.0$ Hz, 2H), 7.79 (m, 1H), 7.73 (d, $J=4.0$ Hz, 1H), 7.60 (d, $J=8.0$ Hz, 1H), 7.46 (d, $J=8.0$ Hz, 2H), 7.11 (t, $J=8.0$ Hz, 1H), 6.54 (dd, $J=4.0$, 12.0 Hz, 1H), 6.36 (t, $J=8.0$ Hz, 1H), 5.27 (s, 2H), 4.57 (d, $J=4.0$ Hz, 2H).

N-(4-((2-aminophenyl)carbamoyl)benzyl)-1*H*-indole-5-carboxamide (**3c**): Mp 177.0–178.2°C. ESI-MS (*m*/*z*): calcd. for $C_{23}H_{20}N_4O_2$ $[M+H]^+$ 385.1586; found 385.1646. ^{1}H NMR (400 MHz, DMSO-d_6) δ 11.26 (s, 1H), 9.57 (s, 1H), 8.90 (t, $J=6.0$ Hz, 1H), 8.19 (s, 1H), 7.93 (d, $J=8.4$ Hz, 2H), 7.68 (dd, $J=1.6$ Hz, 8.4 Hz, 2H), 7.43 (m, 4H), 7.17 (d, $J=7.6$ Hz, 1H), 6.97 (dt, $J=1.2$ Hz, 8.4 Hz, 1H), 6.60 (dt, $J=1.2$ Hz, 8.4 Hz, 1H), 6.54 (d, $J=3.2$ Hz, 1H), 4.81 (s, 2H), 4.56 (d, $J=5.6$ Hz, 2H).

N-(4-((2-amino-4-fluorophenyl)carbamoyl)benzyl)-1*H*-indole-5-carboxamide (**3d**): Mp 188.6–190.1°C. ESI-MS (*m*/*z*): calcd. for $C_{23}H_{19}FN_4O_2$ $[M+H]^+$ 403.1492; found 403.1558. ^{1}H NMR (400 MHz, DMSO-d_6) δ 11.26 (s, 1H), 9.68 (s, 1H), 8.92 (t, $J=6.0$ Hz, 1H), 8.19 (s, 1H), 8.10 (s, 1H), 7.92 (d, $J=8.0$ Hz, 2H), 7.80 (d, $J=8.0$ Hz, 1H), 7.68 (dd, $J=1.6$ Hz, 8.4 Hz, 2H), 7.44 (m, 4H), 6.55 (s, 1H), 5.12 (s, 2H), 4.57 (d, $J=5.6$ Hz, 2H).

N-(4-((2-aminophenyl)carbamoyl)benzyl)-2-methyl-1*H*-benzo[*d*]imidazole-5-carboxamide (**3e**): Mp 225.2–227.0°C. ESI-MS (*m*/*z*): calcd. for $C_{23}H_{21}N_5O_2$ $[M+H]^+$ 400.1695; found 400.1723. ^{1}H NMR (400 MHz, DMSO-d_6) δ 9.64 (s, 1H), 8.13 (s, 1H), 7.93 (m, 4H), 7.73 (d, $J=8.0$ Hz, 1H), 7.55 (d, $J=8.0$ Hz, 1H), 7.45 (m, 3H), 6.97 (d, $J=8.0$ Hz, 1H), 6.78 (d, $J=8.0$ Hz, 1H), 6.60 (t, $J=8.0$ Hz, 1H), 4.92 (s, 2H), 4.55 (d, $J=6.0$ Hz, 2H), 3.35 (s, 3H).

N-(4-((2-amino-4-fluorophenyl)carbamoyl)benzyl)-2-methyl-1*H*-benzo[*d*]imidazole-5-carboxamide (**3f**): Mp 222.9–223.2°C. ESI-MS (*m*/*z*): calcd. for $C_{23}H_{20}FN_5O_2$ $[M+H]^+$ 418.1601; found 418.1632. ^{1}H NMR (400 MHz, DMSO-d_6) δ 9.61 (s, 1H), 9.13 (s, 1H), 8.06 (m, 4H), 7.54 (d, $J=8.0$ Hz, 1H), 7.44 (m, 3H), 7.11 (t, $J=8.0$ Hz, 1H), 6.54 (d, $J=4.0$, 12.0 Hz, 1H) 6.36 (t, $J=8.0$ Hz, 1H), 5.23 (s, 2H), 4.55 (d, $J=4.0$ Hz, 2H), 3.35 (s, 3H).

N-(4-((2-aminophenyl)carbamoyl)benzyl)-2-isopropyl-1*H*-benzo[*d*]imidazole-5-carboxamide (**3g**): Mp 231.1–232.1°C. ESI-MS (*m*/*z*): calcd. for $C_{25}H_{25}N_5O_2$ $[M+H]^+$ 428.2008; found 428.2108. ^{1}H NMR (400 MHz, DMSO-d_6) δ 9.64 (s, 1H), 9.09 (s, 1H), 8.14 (s, 1H), 7.95 (d, $J=8.0$ Hz, 2H) 7.74 (d, $J=16.0$ Hz, 1H), 7.57 (d, $J=4.0$ Hz, 1H), 7.44 (d, $J=8.0$ Hz, 3H), 7.15 (d, $J=8.0$ Hz, 1H), 6.98 (t, $J=8.0$ Hz, 1H), 6.78 (d, $J=8.0$ Hz, 1H), 6.60 (t, $J=8.0$ Hz, 1H), 4.90 (s, 2H), 4.56 (d, $J=8.0$ Hz, 2H), 3.20 (m, 1H), 1.35 (t, $J=8.0$ Hz, 6H).

N-(4-((2-amino-4-fluorophenyl)carbamoyl)benzyl)-2-isopropyl-1*H*-benzo[*d*]imidazole-5-carboxamide (**3h**): Mp 212.3–213.2°C. ESI-MS (*m*/*z*): calcd. for $C_{25}H_{24}FN_5O_2$ $[M+H]^+$ 446.1914; found 446.1944. ^{1}H NMR (400 MHz, DMSO-d_6) δ 9.61 (s, 1H), 9.12 (t, $J=8.0$ Hz, 1H), 8.14 (s, 1H), 7.95 (d, $J=8.0$ Hz, 2H), 7.79 (m, 2H), 7.55 (d, $J=8.0$ Hz, 1H), 7.45 (d, $J=8.0$ Hz, 2H), 7.11 (t, $J=8.0$ Hz, 1H), 6.54 (dd, $J=4.0$, 12.0 Hz, 1H), 6.36 (t, $J=8.0$ Hz, 1H), 5.24 (s, 2H), 4.57 (d, $J=8.0$ Hz, 2H), 3.19 (m, 1H), 1.36 (t, $J=8.0$ Hz, 6H).

N-(4-((2-aminophenyl)carbamoyl)benzyl)-2-(pyridin-3-yl)-1*H*-benzo[*d*]imidazole-5-carboxamide (**3i**): Mp 208.4–210.3°C. ESI-MS (*m*/*z*): calcd. for $C_{27}H_{22}N_6O_2$ $[M+H]^+$ 463.1804; found 463.1760. ^{1}H NMR (400 MHz, DMSO-d_6) δ 9.65 (s, 1H), 9.19 (m, 1H), 8.73 (t, $J=4.0$ Hz, 1H), 8.53 (t, $J=4.0$ Hz, 1H), 8.35 (d, $J=8.0$ Hz, 1H), 8.14 (s, 1H), 7.97 (d, $J=8.0$ Hz, 2H), 7.83 (m, 2H), 7.64 (m, 2H), 7.48 (d, $J=8.0$ Hz, 2H), 7.17 (d, $J=8.0$ Hz, 1H), 6.97 (t, $J=8.0$ Hz, 1H), 6.78 (d, $J=8.0$ Hz, 1H), 6.60 (t, $J=8.0$ Hz, 1H), 4.97 (s, 2H), 4.58 (d, $J=8.0$ Hz, 2H).

N-(4-((2-amino-4-fluorophenyl)carbamoyl)benzyl)-2-(pyridin-3-yl)-1*H*-benzo[*d*]imidazole-5-carboxamide (**3j**): Mp 179.3–181.6°C. ESI-MS (*m*/*z*): calcd. for $C_{27}H_{21}FN_6O_2$ $[M+H]^+$ 481.1740; found 481.1802. ^{1}H NMR (400 MHz, DMSO-d_6) δ 9.57 (s, 1H), 9.13 (m, 1H), 8.26 (d, $J=8.0$ Hz, 1H), 8.20 (m, 1H), 8.03 (s, 1H), 7.95 (d, $J=8.0$ Hz, 2H) 7.77 (t, $J=8.0$ Hz, 1H), 7.65 (d, $J=8.0$ Hz, 1H), 7.57 (d, $J=8.0$ Hz, 1H), 7.46 (d, $J=8.0$ Hz, 2H), 7.11 (t, $J=8.0$ Hz, 1H), 6.77 (d, $J=8.0$ Hz, 1H), 6.53 (m, 2H), 6.36 (t, $J=8.0$ Hz, 1H), 5.24 (s, 2H), 4.57 (d, $J=4.0$ Hz, 2H).

N-(4-((2-amino-4-fluorophenyl)carbamoyl)benzyl)-2-(6-fluoropyridin-3-yl)-1*H*-benzo[*d*]imidazole-5-carboxamide (**3k**): Mp > 250°C. ESI-MS (*m*/*z*): calcd. for $C_{27}H_{20}F_2N_6O_2$ $[M+H]^+$ 499.1616; found 499.1608. ^{1}H NMR (400 MHz, DMSO-d_6) δ 9.57 (s, 1H), 9.13 (m, 1H), 8.26 (d, $J=8.0$ Hz, 1H), 8.20 (m, 1H), 8.03 (s, 1H), 7.95 (d, $J=8.0$ Hz, 2H), 7.78 (t, $J=8.0$ Hz, 1H), 7.65 (d, $J=8.0$ Hz, 1H), 7.54 (d, $J=8.0$ Hz, 1H), 7.46 (d, $J=8.0$ Hz, 2H), 7.11 (t, $J=8.0$ Hz, 1H), 6.53 (m, 2H), 6.36 (t, $J=8.0$ Hz, 1H), 5.29 (s, 2H) 4.59 (d, $J=4.0$ Hz, 2H).

N-(4-((2-aminophenyl)carbamoyl)benzyl)-2-(6-fluoropyridin-3-yl)-1*H*-benzo[*d*]imidazole-5-carboxamide (**3l**): Mp 249.2–251.4°C. ESI-MS (*m*/*z*): calcd. for $C_{27}H_{21}FN_6O_2$ $[M+H]^+$ 481.1710; found 481.1804. ^{1}H NMR (400 MHz, DMSO-d_6) δ 9.66 (s, 1H), 9.15 (t, $J=8.0$ Hz, 1H), 8.27 (d, $J=8.0$ Hz, 1H), 8.20 (dd, $J=4.0$ Hz, 8.0 Hz, 1H), 8.11 (s, 1H), 7.96 (d, $J=8.0$ Hz, 2H), 7.80 (t, $J=8.0$ Hz, 1H), 7.65 (d, $J=4.0$ Hz, 1H), 7.55 (d, $J=8.0$ Hz, 1H), 7.45 (d, $J=12.0$ Hz, 2H), 7.17 (d, $J=8.0$ Hz, 1H), 6.98 (t, $J=8.0$ Hz, 1H), 6.79 (d, $J=8.0$ Hz, 1H), 6.60 (t, $J=8.0$ Hz, 1H), 6.54 (d, $J=12.0$ Hz, 1H), 4.91 (s, 2H) 4.59 (d, $J=8.0$ Hz, 2H).

N-(4-((2-amino-4-fluorophenyl)carbamoyl)benzyl)-2-(4-fluorophenyl)-1*H*-benzo[*d*]imidazole-5-carboxamide (**3m**): Mp 189.3–190.4°C. ESI-MS (*m*/*z*): calcd. for $C_{28}H_{21}F_2N_5O_2$ $[M+H]^+$ 498.1663; found 498.1758. ^{1}H NMR (400 MHz, DMSO-d_6) δ 9.58 (s, 1H), 9.15 (m, 1H), 8.27 (t, $J=8.0$ Hz, 2H), 8.10 (s, 1H), 7.96 (d, $J=8.0$ Hz, 2H), 7.83 (t, $J=8.0$ Hz, 1H), 7.73 (d, $J=8.0$ Hz, 1H), 7.60 (d, $J=8.0$ Hz, 1H), 7.46 (m, 4H), 7.11 (t, $J=8.0$ Hz, 1H), 6.54 (dd, $J=4.0$,12.0 Hz, 1H), 6.36 (t, $J=8.0$ Hz, 1H), 5.24 (s, 2H), 4.59 (d, $J=4.0$ Hz, 2H).

N-(4-((2-aminophenyl)carbamoyl)benzyl)-2-(4-fluorophenyl)-1*H*-benzo[*d*]imidazole-5-carboxamide (**3n**): Mp 237.6–238.5°C. ESI-MS (*m*/*z*): calcd. for $C_{28}H_{22}FN_5O_2$ $[M+H]^+$ 480.1758; found 480.1801. ^{1}H NMR (400 MHz, DMSO-d_6) δ 9.65 (s, 1H), 9.17 (s, 1H), 8.26 (t, $J=8.0$ Hz, 2H), 8.12 (s,

1H), 7.95 (m, 2H), 7.83 (d, $J = 8.0$ Hz, 1H), 7.66 (d, $J = 4.0$ Hz, 1H), 7.45 (m, 5H), 7.17 (d, $J = 8.0$ Hz, 1H), 6.97 (t, $J = 8.0$ Hz, 1H), 6.78 (d, $J = 8.0$ Hz, 1H), 6.60 (t, $J = 8.0$ Hz, 1H), 4.92 (s, 2H), 4.60 (d, $J = 4.0$ Hz, 2H)

Fluorescence Assay of HDAC Inhibition Activities

In vitro HDAC inhibition assays were performed as previously described.[13] In brief, 10 µL of enzyme solution (HeLa cell nuclear extract, HDAC1, HDAC2, HDAC6, or HDAC8, obtained from BPS Bioscience, San Diego, California, United States) was mixed with different concentrations of the tested compound (50 µL). The mixture was incubated at 37°C for 5 minutes, followed by adding 40 mL of the fluorogenic substrate. The substrate Boc-Lys(Acetyl)-AMC (Bidepharm, Shanghai, China) was used for assaying HDAC1, HDAC2 and HDAC6; and boc-lys(triflouroacetyl)-AMC (Bidepharm, Shanghai, People's Republic of China) was used for assaying HDAC8. After incubation at 37°C for 30 minutes, the mixture was quenched by 100 µL of the developer containing trypsin and trichostatin A, and incubated for another 20 minutes. Fluorescence intensity was measured using SpectraMax M5 (Molecular Devices, LLC., San Jose, California, United States) at excitation wavelengths of 390 nm and emission wavelengths of 460 nm. The inhibition ratios were calculated from the fluorescence intensity readout of tested wells relative to those of control wells, and the IC_{50} values were calculated using the Prism nonlinear curve fitting method (allowed to float and fitted as a parameter).

Cell Culture

PC-3, HT-29, HCT-116, SK-BR-3, Jurkat E6–1, A549, Colo205, MCF-7, and MRC-5 cells (ATTC, United States) were maintained in Roswell Park Memorial Institute 1640 medium (Thermo Fisher Scientific, Waltham, Massachusetts, United States) containing 10% fetal bovine serum (EXCELL, Catalog #: FND500, Australia) at 37°C in a 5% CO_2 humidified incubator. Cells were ported into a 96-well cell plate, and allowed to grow for 12 hours before the experiments.

In Vitro Antiproliferative Assay

The 3-[4,5-dimethyl-2-thiazolyl]-2,5-diphenyl-2*H*-tetrazolium bromide (MTT) method was used to assess cell proliferation according to the manufacturer's instructions. Cells were treated with different concentrations of compounds for 48 hours. Then, 0.5% MTT solution was added to each well. After incubation for another 4 hours, formazan formed from MTT was extracted by adding 200 µL of DMSO. Absorbance values correlate well with cell proliferation and was determined using a multilabel reader (EnVision, PerkinElmer, United States) at the wavelength of 570 nm.

Molecular Modeling Study

The docking was conducted in Glide module of Schrodinger Maestro. The PDB entry 4BKX downloaded from Protein Data Bank (https://www.rcsb.org/structure/4BKX) for molecular docking. In Protein Preparation Wizard, the HDAC1 protein was prepared by the process of removing water and adding hydrogens. The most important of resulting structure was refined in the force field of OPLS3 with the hydrogen only. Then, the Receptor Grid Preparation was defined according to the position of the zinc ion. Compound **3c** generated all possible combinations at the target pH 7.0 ± 2.0 in the force field of OPLS3 in LigPrep module. Ligand docking parameter was set default. Molecular docking result was generated using PyMol (http://pymol.sourceforge.net/).

Compound on hERG Activity

Whole-cell recordings were performed using automated Qpatch (Sophion, Biolin Scientific, Stockholm, Sweden). Cells were voltage clamped at a holding potential of −80 mV. The hERG current was activated by depolarizing at +20 mV for 5 seconds, after which the voltage was taken back to −50 mV for 5 seconds to remove the inactivation and observe the deactivating hERG tail current. The voltage stimulation was applied per 15 seconds. Compound solutions were administrated from low to high concentration with 2 minutes for each concentration, and 10 µmol/L cisapride was applied at the end of perfusion of compound solution. Each concentration was tested on at least three parallels. The degree of hERG channel inhibition was determined by the following equation: Inhibition (%) = (1 − variation in the current before and after addition of a test substance/variation in the current before and after addition of a medium) × 100.

In Vivo Bioavailability Study (Pharmacokinetic Parameter)

Male SD rats ($n = 3$) were purchased form SLRC laboratory Animal Inc., Shanghai, People's Republic of China, and used in the pharmacokinetic parameter studies of compound **3c.** Compound **3c** was dissolved and vortexed in 5% DMSO, 10% Tween 80, and 75% physiological saline for a concentration of 0.2 and 1 mg/mL. Rats were housed in a room with controlled temperature and humidity and allowed free access to food and water. The rats were split into iv group (2 mg/kg) and ig group (10 mg/kg) before starting treatment (24 rats in each group). At indicated time points, blood was collected from rats at various time points up to 12 hours. The concentrations of compounds in plasma were determined by LC/MS/MS (Shimadzu LC-30AD, Kyoto Japan). A solution of 0.05 N HCl in saline was used as the vehicle.

In Vivo Antitumor Activity Assay

The antitumor effect of compound **3c** was assessed in a mouse xenograft HCT116 tumor model. Female BALB/C mice (6 weeks old) were purchased form SLRC laboratory Animal Inc. and housed and maintained under specific-pathogen free conditions. Animal procedures were performed according to institutional ethical guidelines of animal care. The HCT-116 cells (5×10^7/mL) in logarithmic growth phase were suspended with Geltrex. The cell suspension (120 µL) was injected subcutaneously into the right flank of mice with a 1 mL syringe. The tumor in mice was observed regularly until reaching to 100–300 mm^3. Then the tumor-bearing mice ($n = 40$) were randomly divided into four groups: vehicle control group ($n = 16$) and three test substance groups ($n = 8$). Vehicle groups were given vehicle alone. The treatment groups were given **3**c (ig) once a day for 21 days at a dose of 45, 80, and 150 mg/kg, respectively .

The tumor diameter was measured twice a week, and the tumor volume was calculated as the following: $V = [\text{length (mm)} \times \text{width}^2\ (\text{mm}^2)]/2$.

Ethics Statement

The present study was approved by the animal ethics committee and abides by the relevant agreements of China State Institute of Pharmaceutical Industry, Shanghai, People's Republic of China.

Funding

This work was financially supported by the National Science and Technology Major Project (Grant No. 2018ZX09711002-002-009), the National Natural Science Foundation of China (Grant No. 81703358), and the Science and Technology Commission of Shanghai Municipality (Grant Nos. 22ZR1460300, 18QB1404200, and 21S11908000).

Conflict of Interest

All authors declare no conflict of interest.

References

1 Marks P, Rifkind RA, Richon VM, Breslow R, Miller T, Kelly WK. Histone deacetylases and cancer: causes and therapies. Nat Rev Cancer 2001;1(03):194–202
2 Zagni C, Floresta G, Monciino G, Rescifina A. The search for potent, small-molecule HDACIs in cancer treatment: a decade after vorinostat. Med Res Rev 2017;37(06):1373–1428
3 Falkenberg KJ, Johnstone RW. Histone deacetylases and their inhibitors in cancer, neurological diseases and immune disorders. Nat Rev Drug Discov 2014;13(09):673–691
4 Bassett SA, Barnett MP. The role of dietary histone deacetylases (HDACs) inhibitors in health and disease. Nutrients 2014;6(10): 4273–4301
5 Engel JA, Jones AJ, Avery VM, et al. Profiling the anti-protozoal activity of anti-cancer HDAC inhibitors against Plasmodium and Trypanosoma parasites. Int J Parasitol Drugs Drug Resist 2015;5 (03):117–126
6 Piekarz R, Bates S. A review of depsipeptide and other histone deacetylase inhibitors in clinical trials. Curr Pharm Des 2004;10 (19):2289–2298
7 Kelly WK, Richon VM, O'Connor O, et al. Phase I clinical trial of histone deacetylase inhibitor: suberoylanilide hydroxamic acid administered intravenously. Clin Cancer Res 2003;9(10, Pt 1):3578–3588
8 Ruiz R, Raez LE, Rolfo C. Entinostat (SNDX-275) for the treatment of non-small cell lung cancer. Expert Opin Investig Drugs 2015;24 (08):1101–1109
9 Ning ZQ, Li ZB, Newman MJ, et al. Chidamide (CS055/HBI-8000): a new histone deacetylase inhibitor of the benzamide class with antitumor activity and the ability to enhance immune cell-mediated tumor cell cytotoxicity. Cancer Chemother Pharmacol 2012;69(04):901–909
10 Stumpp HH, Bracker TU, Henderson D, et al. MS-275, a potent orally available inhibitor of histone deacetylases-the development of an anticancer agent. Biochem Cell Biol 2007;39(07): 1388–1405
11 Finnin MS, Donigian JR, Cohen A, et al. Structures of a histone deacetylase homologue bound to the TSA and SAHA inhibitors. Nature 1999;401(6749):188–193
12 Liang X, Zang J, Li X, et al. Discovery of novel Janus kinase (JAK) and histone deacetylase (HDAC) dual inhibitors for the treatment of hematological malignancies. J Med Chem 2019;62(08): 3898–3923
13 Zhang Z, Zhang Q, Zhang H, et al. Discovery of quinazolinyl-containing benzamides derivatives as novel HDAC1 inhibitors with in vitro and in vivo antitumor activities. Bioorg Chem 2021;117:105407–105418
14 Wang H, Yang C, Doherty JR, Roush WR, Cleveland JL, Bannister TD. Synthesis and structure-activity relationships of pteridine dione and trione monocarboxylate transporter 1 inhibitors. J Med Chem 2014;57(17):7317–7324